View metadata, citation and similar papers at core.ac.uk

brought to you by CORE

provided by Caltech Authors - Main

PROCEEDINGS OF SPIE

SPIEDigitalLibrary.org/conference-proceedings-of-spie

New insights into the nature of the circumstellar environment of FU Ori

Jean-Philippe Berger, Fabien Malbet, M. Mark Colavita, Damien Segransan, Rafael Millan-Gabet, et al.

Jean-Philippe Berger, Fabien Malbet, M. Mark Colavita, Damien Segransan, Rafael Millan-Gabet, Wesley A. Traub, "New insights into the nature of the circumstellar environment of FU Ori," Proc. SPIE 4006, Interferometry in Optical Astronomy, (5 July 2000); doi: 10.1117/12.390259

SPIE.

Event: Astronomical Telescopes and Instrumentation, 2000, Munich, Germany

Downloaded From: https://www.spiedigitallibrary.org/conference-proceedings-of-spie on 7/11/2018 Terms of Use: https://www.spiedigitallibrary.org/terms-of-use

New insights in the nature of the circumstellar environment of FU Ori

Jean-Philippe Berger[a,b], Fabien Malbet[b], Mark M. Colavita[c], Damien Ségransan[b], Rafael Millan-Gabet[d], and Wes Traub[d]

[a] Laboratoire d'Électromagnétisme Microondes et Optoélectonique, ENSERG, BP 257, F-38016 Grenoble cedex 1, France

[b] Laboratoire d'Astrophysique, Observatoire de Grenoble, UMR CNRS/UJF 5571 BP 53, F-38041, Grenoble Cedex 9, France

[c] Jet Propulsion Laboratory, California Institute of Technology 4800 Oak Grove Drive, CA 91109 Pasadena, USA

[d] Smithsonian Astrophysical Observatory, Center for Astrophysics Garden Street, MA 02138

ABSTRACT

Following a previous succesful study, we present new and more complete interferometric observations of FU Orionis. The combination of both IOTA (*Infrared and Optical Telescope Array,* Mt Hopkins, AZ) and PTI (*Palomar Testbed Interferometer*, Palomar Observatory, CA) interferometers allowed an increase in (u, v) coverage and H and K bands measurements. We confirm the presence of a resolved structure around FU Ori that can be interpreted in terms of accretion disk. However, we find significant differences between our results and standard accretion disks models. In particular the temperature power law is best explained if two different radial regimes are used. Moreover, a clear visibility oscillation trend at 110 m is well fitted with a binary (or hot spot) model. This may have important implications on accretion disk models for such objects.

Keywords: Interferometry, infrared, young stellar objects, circumstellar matter

1. PROBING THE INNER PART OF AN ACCRETION DISK

Malbet & Bertout[1] predicted that long-baseline interferometry would be able to detect thermal emission from accretion disks around young stars in the near infrared. The increase in sensitivity of infrared interferometers allowed Malbet et al.[2] (paper I) to resolve **FU Orionis** at the AU scale with the PTI interferometer (PTI, Palomar Observatory, CA), this was the first time ever such resolutions were attained on such objects. These observations were shown to be compatible with standard accretion disk interpretations[3]. However, the limited precision of the measurements and limited (u, v) coverage forbid more detailed information on the physical mechanisms operating close to the central star to be obtained. Further observing runs have therefore been carried out since at two of the existing infrared interferometers, the *Palomar Testbed Interferometer* (PTI, Palomar Observatory, CA) and the *Infrared and Optical Telescope Array* (IOTA, Mt Hopkins, AZ), in order to further address the question of the close environment of Young Stellar Objects (YSOs). These new results are the subject of this paper.

2. FU ORIONIS

FU Orionis is the prototype of a class of YSO called FU Orionis stars (FU ors), that have undergone photometric outbursts on the order of 4-6 mag in less than 1 yr[4]. Table 1 summarizes FU Orionis's main observational properties.

A FU Orionis star's luminosity typically peaks at $500L_{\odot}$ and then decays on a 100 yr timescale. FU Orionis stars exhibit large infrared excesses, double-peaked line profiles, apparent spectral types that vary with wavelength, broad and blueshifted Balmer absorption line, and are often associated with strong mass outflows (see Hartmann & Kenyon[5] for a recent review on this phenomenon).

In *Interferometry in Optical Astronomy*, Pierre J. Léna, Andreas Quirrenbach, Editors,
Proceedings of SPIE Vol. 4006 (2000) • 0277-786X/00/$15.00

Downloaded From: https://www.spiedigitallibrary.org/conference-proceedings-of-spie on 7/11/2018
Terms of Use: https://www.spiedigitallibrary.org/terms-of-use

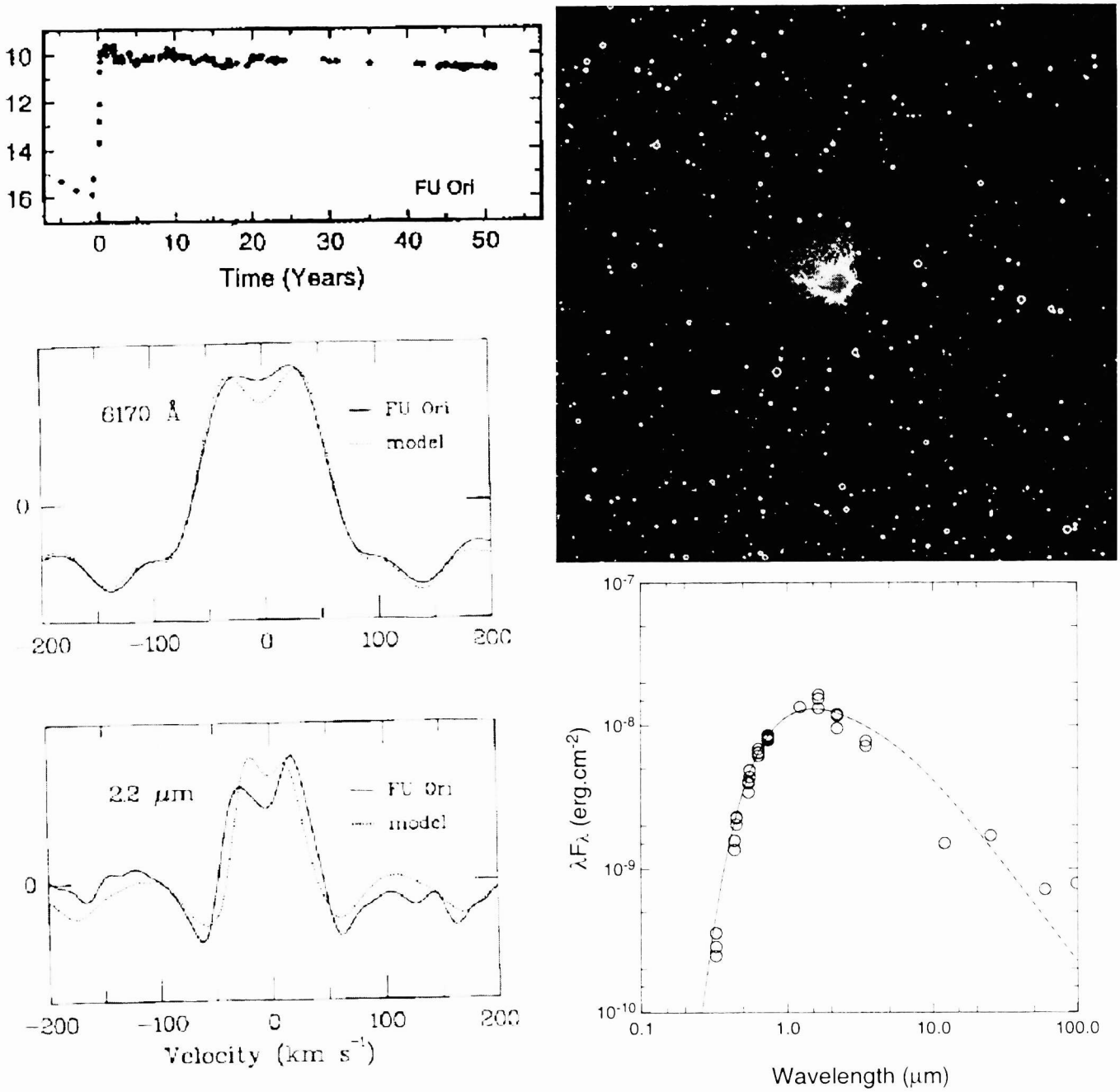

Figure 1. Upper left: optical B photometry outburst and decline of FU Ori[5]. Upper right: image from the Digital Sky Survey (10×10 arcmin). Lower left: comparison of observed and accretion disk model line cross-correlations at 6170 A and 2.2 μm[6]. Lower right: spectral energy distribution from literature data[6–8](circles) and IRAS, from our accretion disk model (dashed line), the star (dotted line) and the whole system (solid line).

Downloaded From: https://www.spiedigitallibrary.org/conference-proceedings-of-spie on 7/11/2018
Terms of Use: https://www.spiedigitallibrary.org/terms-of-use

Table 1. FU Orionis properties see Hartmann & Kenyon[5] for a recent review.

Location	Orion
Object type	FUor
Distance	450 pc
Luminosity	$L \sim 500$ $L_\odot$
Extinction	$A_V \sim 1-3$ mag
Magnitudes	$V = 8.9$, $R = 7.7$, $K = 4.6$ mag
Variability	4-6 mag amplitude
	outburst + decay ($t \sim 100$ yr)
Spectrophotometry	large infrared excess
Spectral type	F2I[9]
	From F7I (λ3860) to <K3 (λ7050)
HR spectroscopy	broad, blueshifted Balmer line absorption
	double-peaked line profiles
Reflection nebula	60 arcsec wide[10]
Scattering envelope	73 mas resolved by speckle
	or unresolved[11]?
Outflows	no CO flow, no jet

3. OBSERVATIONS

FU Orionis was observed with IOTA from December, 13, 1998 to December, 26, 1998 using two baselines: the 38 m baseline oriented North-Northeast and the 21m North-South baseline. We used H and K' filters. FU Orionis was observed with PTI during three campaigns, 1997 (data published in paper I), 1998 (from November, 14, 1998 to November, 27, 1998) and 1999 (from November, 23, 1999 to December 1, 1999). Data obtained during the two latter campaigns are published in this paper. 1998 observations were made with the K filter and 1999 with both H and K filters.

Several calibrators were used for these observations, described as follows. All calibrators were used for IOTA observations and calibrators in bold face were also used at PTI. Following the source name, we indicate in parenthesis the angular diameter in milliarcseconds (mas), estimated from Hipparcos data: **HD42807 (0.48)**, HD38529 (0.38), HD31295 (0.53), **HD37147 (0.34)**, HD30739 (0.45), HD46241 (0.41), HDC35956 (0.35), HDC42618 (0.38), HDC43683 (0.18), HDC43931(0.21). HD35296 (0.70) was only used at PTI.

The observation period on both interferometers was long enough to allow the projected baseline on sky to rotate with a significant hour angle range ($[-2.8, +0.6]$ for the PTI observations and $[-0.6, +4.4]$ for the IOTA observations).

4. DATA PROCESSING

PTI data processing is described in Colavita[12]. The visibility estimation is based upon the ABCD algorithm. Out of the four estimators available we have choosen the incoherent spectral estimator. The spectrometer has an higher instrumental transfer function because of the spatial filtering effect of the single mode fiber. The incoherent estimator allows to average visibilities over the entire H and K band without introducing biases due to atmospheric piston (cf. paper I).

The IOTA interferometer temporally encodes fringes. We have choosen to use a quadratic estimator similar to the one described in Foresto et al.[13] with no photometric calibration signals available. The two output interferograms recorded simultaneously are substracted to construct a single interferogram with reduced photometric contamination*. For each batch of 500 scans an average visibility is computed. The standard deviation of this batch provides the error estimation on this measurement. Visibility is computed by estimating the energy contained at the fringe position in the spectral power density.

*As the fringes are π shifted this leads to maximizing the energy in the spectral density distribution at the fringe position and reducing the photometric energy at lower frequencies.

Downloaded From: https://www.spiedigitallibrary.org/conference-proceedings-of-spie on 7/11/2018
Terms of Use: https://www.spiedigitallibrary.org/terms-of-use

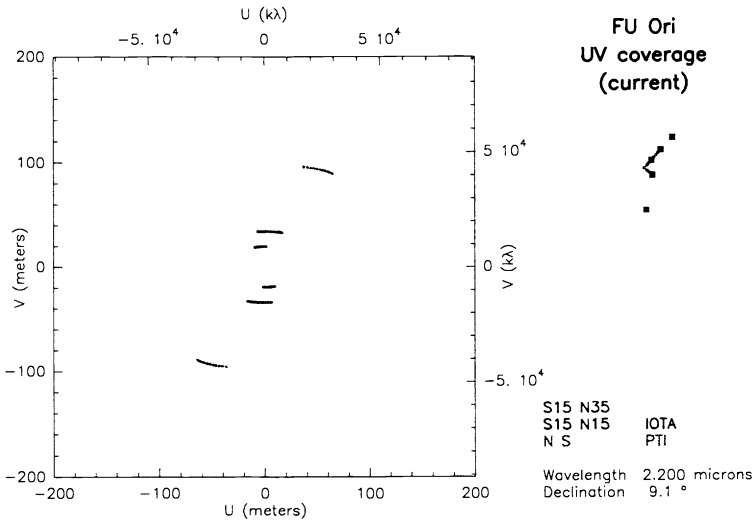

Figure 2. FU Orionis (u, v) coverage corresponding to the observations of this paper.

Once the raw visibilities are derived for the data from each interferometer separately, data reduction enters the calibration part, which is common to both data sets. The key point is to estimate the instrumental visibility by observing calibrators located near the source in angle. For each FU Ori visibility we compute an instrumental visibility. Division of both quantities leads to the determination of the unbiased visibility and its associated error. Calibrators are corrected for the intrinsic visibility loss due to their angular diameter. All calibrators measurements made within half an hour, before and after a target measurement are included in the instrumental visibility estimation. We then compute a weighted average of all calibrators visibilities in that interval with a weight equal to the inverse of the time delay between the calibrator measurement and the target measurement.

5. THE RESULTS

These new observations extend the (u, v) coverage of paper I (see Fig. 2) to smaller baselines and to the H band. Calibrated visibilities are presented in Fig. 3. The calibrated squared visibilities of FU Ori at 110m in K band display a clear oscillation trend. Note that IOTA K' squared visibilities at 21m are smaller than at 38 m. IOTA data are derived by a first version of data reduction, and error bars are certainly overestimated. An improved statistical processing should allow the refinement of our fits. Globally we distinguish three trends in the whole set of data:

- a global average decrease of visibility with increasing projected baseline (except when comparing 21m and 38 m IOTA baselines K' data, see discussion below).
- superimposed oscillations at the 110 m PTI baseline.
- 21m K' band visibility is smaller than 38m visibility.

6. INTERPRETATION

FUors have been convincingly modeled as low-mass pre-main sequence stars (T Tauri stars) which are surrounded by luminous and active accretion disks. The inferred peak accretion rates are on the order of 10^{-4} $M_\odot$ yr^{-1}. The energy released by the accretion process is radiated at the disk surface, overwhelming the stellar emission. The disk paradigm allows to explain many exotic features of FUors[5].

In this global context we try to interpret both observed trends as the consequence of an accretion disk surrounding a primary star with the presence of a secondary companion.

Downloaded From: https://www.spiedigitallibrary.org/conference-proceedings-of-spie on 7/11/2018
Terms of Use: https://www.spiedigitallibrary.org/terms-of-use

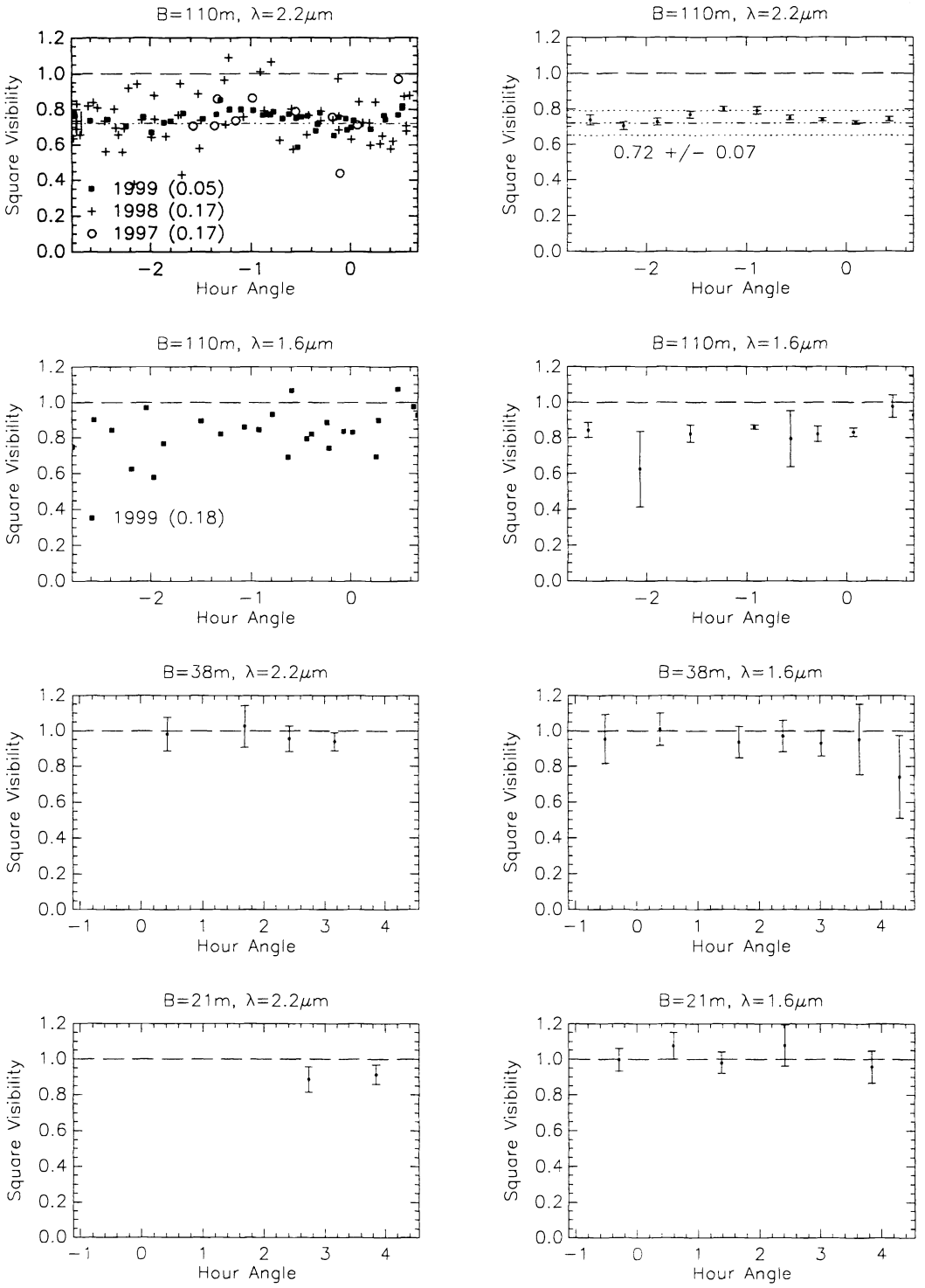

Figure 3. Calibrated square visibilities of FU Ori as a function of hour angle. **First row :** PTI data K band; left figure displays all the visibilities obtained during a three year campaign 1997 (circles), 1998 (crosses), 1999 (squares) typical average errors for each point are quoted (in parenthesis); right figure displays binned data with corresponding error bars. Dashed dotted lines represent results from paper I (average and standard deviation limits). **Second row :** PTI data H band; left figure displays the 1999 visibilitities, right figure the corresponding binned visibilities. **Third row :** IOTA data K' and H bands at 38 m; binned visibilities. **Fourth row :** IOTA data K' and H bands at 21 m; binned visibilities.

Downloaded From: https://www.spiedigitallibrary.org/conference-proceedings-of-spie on 7/11/2018
Terms of Use: https://www.spiedigitallibrary.org/terms-of-use

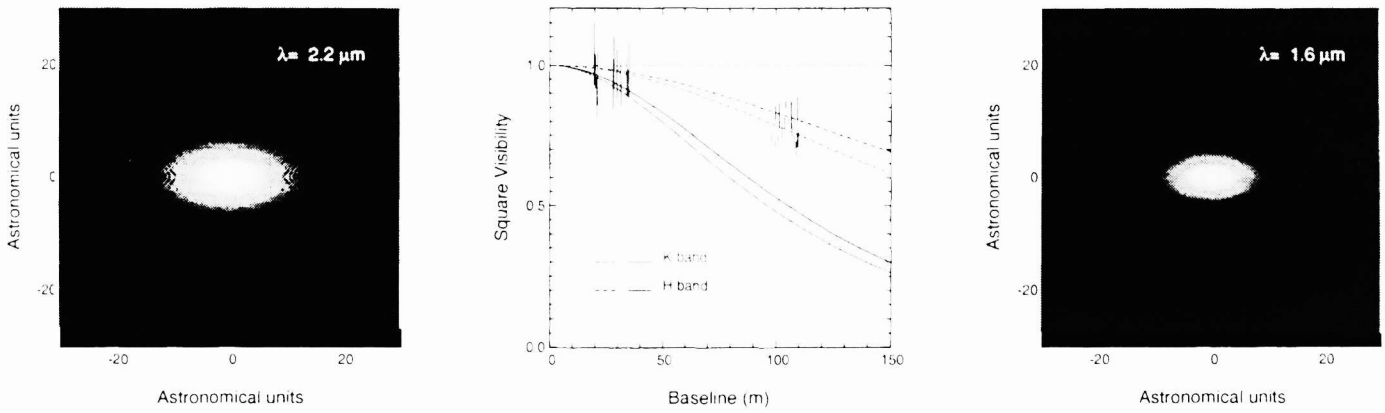

Figure 4. Result of the fit of an accretion disk model on our data. Central figure shows squared visibilities as a function of projected baseline. Red curves show the expected variation for K band squared visibilities for two perpendicular orientations (solid and dashed lines). Blue curves show the expected variation for H band squared visibilities for two perpendicular orientations (solid and dashed lines). Right and left figures display synthetic image reconstructions at K and H bands obtained with the derived parameters (see text section 6.1).

6.1. The accretion disk scenario

Standard accretion disk models predict that temperature varies as a power of the radius, $T \sim r^{-q}$; where $q = 0.75$. We have fitted average visibilities at each baselines and wavelength with this model **and** FU Ori spectral energy distribution (SED). The resulting SED fit can be seen in Fig. 1 and the visibility fit in Fig. 4. We found that the squared visibility variation cannot be reproduced with a single power law. We need a double power law distribution to obtain satisfying fits. This leads to the following main disk characteristics: inner radius = 13 solar radius, outer radius = $400AU$, accretion rate = $8 \times 10^{-5} M_\odot$/yr, inclination angle = $60°$, $q \sim 0.6$ between 0 and 2.5 AU and $q \sim 0.75$ in the external parts. Figure 4 displays two synthetic images of the derived accretion disks for 1.6μm and 2.2μm.

A first attempt to explain this behaviour could lead to a link between accretion and ejection processes. We expect the ejection process to significantly change the accretion in the inner part of the disk.

6.2. The influence of a secondary unresolved companion

We have tried to link oscillations observed at 110 m with the presence of a point source companion. We used a preliminary model consisting of a gaussian brightness distribution profile (to simulate the disk influence and consequently account for the 110 m average visibility) + an unresolved companion located next to the gaussian envelope. Fit results can be seen in Fig. 5. Although deeper checks should be made, the main result of this modelization is that this is the best way to explain oscillations at 110 meters. The fit lead to a reduced $\chi^2 \leq 1$. Moreover, this simple scenario is sufficient to explain that the K' band squared visibilities are lower at 21 m than at 38 m (third trend) since oscillations are present at all spatial frequencies. The main characteristics of this secondary companion are $\Delta K \sim 3.8$, $\Delta H \sim 5.2$, $s = 36.5$mas and $PA = 165°$ where $\Delta K, \Delta H$ are the magnitudes differences with the resolved source at H and K bands, s stands for separation and PA for position angle. These magnitudes correspond to a companion redder than a standard T Tauri star, and the separation corresponds to 12 AU at the FU Ori distance. The separation is at the limiting resolution of the greatest monolithic telescopes, yet the magnitude difference should make it hard to directly image. The presence of a hot spot at the disk surface could also explain such observations. However, given its separation from the central source it would be located at distances were temperature has significantly dropped. Physical mechanisms explaining such a local temperature elevation at theses distances are still to be found.

7. CONCLUSION

We have observed FU Orionis with long-baseline interferometry in the near-infrared, achieving a projected spatial resolution of 2 AU using the *Palomar Testbed Interferometer* and the *Infrared Optical Telescope Array*. The (u, v)

Downloaded From: https://www.spiedigitallibrary.org/conference-proceedings-of-spie on 7/11/2018
Terms of Use: https://www.spiedigitallibrary.org/terms-of-use

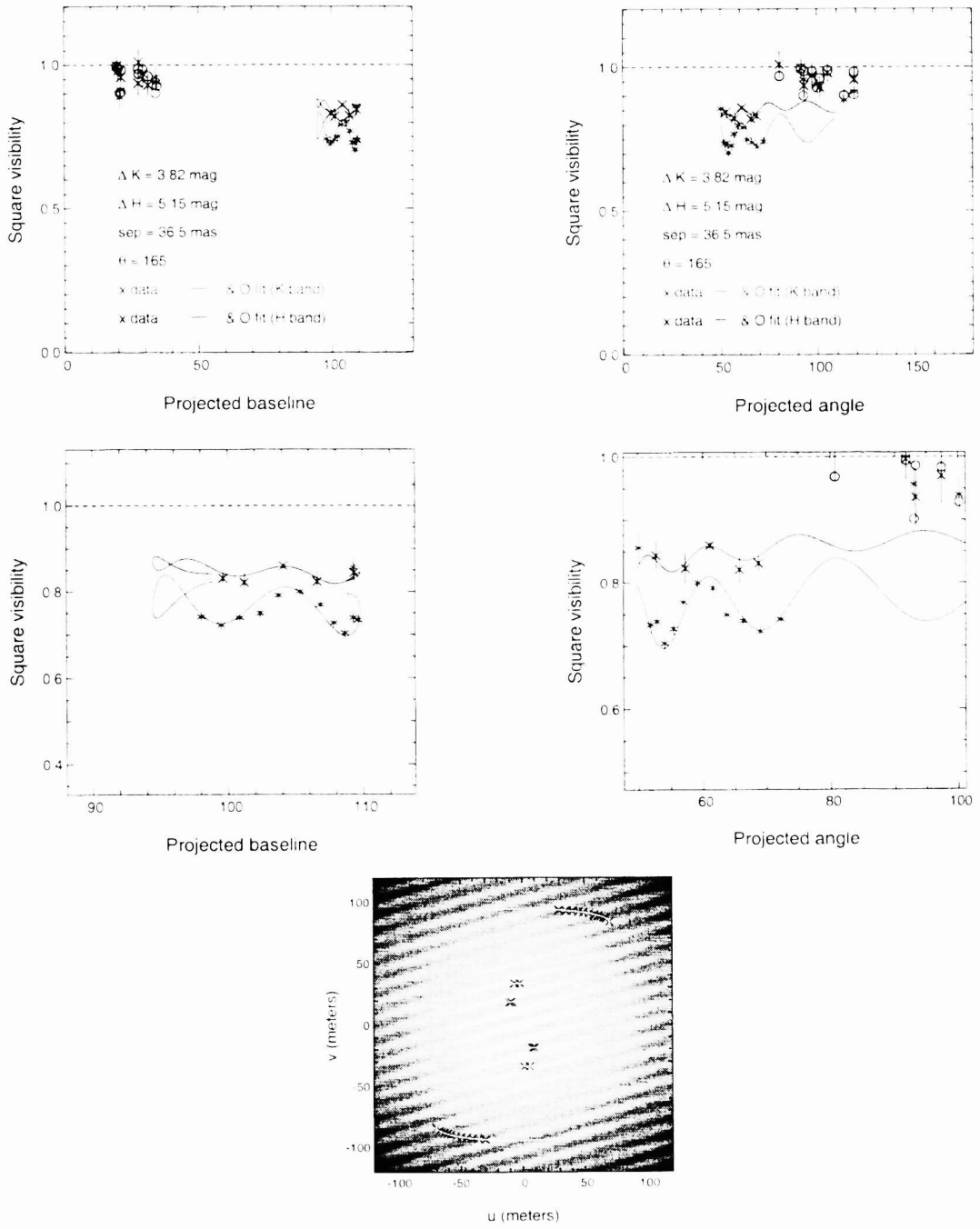

Figure 5. Results of a data fit with a gaussian symmetric brightness profile + binary companion model. Dark colors concern the H band, grey colors the K band. **Left column top and bottom :** Squared visibilities as a function of projected baseline. Crosses indicate data points, circles and lines result of the model fit. Curves have been computed for a time range greater than the observation time (HA range $=[-4,4]$). This explains why curves are more extended than data points. Second row panels show a zoom on the 110-m oscillation. **Right column top and bottom :** Squared visibilities as a function of projected angle. Bottom figure shows a zoom on the 110 oscillation. **Center bottom column :** 2D squared visibility of the fit has been displayed. Both the large scale decrease and the binary oscillations are clearly visible. The observational (u,v) coverage can be seen as red crosses. White lines are the expected (u,v) coverage with an extended observational time (HA range $=[-4,4]$).

Downloaded From: https://www.spiedigitallibrary.org/conference-proceedings-of-spie on 7/11/2018
Terms of Use: https://www.spiedigitallibrary.org/terms-of-use

coverage provided by Earth rotation and the precision were significant enough to detect oscillations in the squared visibility variation. We found that these observations can be explained if FU Orionis is a binary star with one component at least containing an accretion disk. The main properties we derived for the accretion disk component points to a deviation from the standard model in the inner part of the disk, and clearly motivates further detailed modeling. In particular, a significant change in the temperature radial distribution has been discovered. One explanation could be the influence of an ejection process. A full fit of all the observables with an improved data reduction and several astrophysical scenari is under progress and will be presented in a forthcoming paper.

References

1. F. Malbet, and C. Bertout, "Detecting T Tauri disks with optical long-baseline interferometry," *A&AS* **113**, pp. 369-xxx, 1995.
2. F. Malbet, J.-P. Berger, M.M. Colavita et al., "FU Orionis Resolved by Infrared Long-Baseline Interferometry at a 2 AU Scale," *ApJ Letters* **507**, pp. 149-152, 1998.
3. D. Lynden-Bell, and J.E. Pringle, "The evolution of viscous discs and the origin of the nebular variables.," *MNRAS* **168**, pp. 603-637, 1974.
4. G. Herbig,"" *Vistas Astron* **8**, pp. 109, 1966.
5. L. Hartmann, and S.J. Kenyon, "The FU Orionis Phenomenon," *ARA&A* **34**, pp. 207-240, 1996.
6. S.J. Kenyon, L. Hartmann, and R. Hewett, "Accretion disk models for FU Orionis and V1057 Cygni - Detailed comparisons between observations and theory," *ApJ* **325**, pp. 231-251, 1988.
7. D.A. Allen, "Near infrared magnitudes of 248 early-type emission-line stars and related objects.," *MNRAS* **161**, pp. 145-166, 1973.
8. I.S. Glass, and M.V. Penston, "An infrared survey of RW Aurigae stars," *MNRAS* **167**, pp. 237-249, 1974.
9. M. Cohen, and L.V. Kuhi, "Observational studies of pre-main-sequence evolution," *ApJ Suppl. Ser.* **41**, pp. 743-843, 1979.
10. T. Nakajima, and D.A. Golimowski, "Coronagraphic imaging of pre-main-sequence stars: Remnant envelopes of star formation seen in reflection," *AJ* **109**, pp. 1181-1198, 1995.
11. L.E. DeWarf, and H.M. Dyck, "The infrared morphology of young stellar objects without companions - A speckle interferometric study," *AJ* **105**, pp. 2211-2225, 1993.
12. M. Colavita, "Fringe Visibility Estimators for the Palomar Testbed Interferometer" *PASP* **111**, pp. 111-117, 1999.
13. V. Foresto, S. Ridgway, and J. -M. Mariotti, "Deriving visibilities from a fiber stellar interferometer" *A&A Suppl. Ser* **121**, pp. 379-392, 1997.

Downloaded From: https://www.spiedigitallibrary.org/conference-proceedings-of-spie on 7/11/2018
Terms of Use: https://www.spiedigitallibrary.org/terms-of-use